Frontiers in Bioscience Landmark

Front. Biosci. (Landmark Ed) **2026**; 31(7): 53057
https://doi.org/10.31083/FBL53057

Original Research

Downregulation of *PHB1* due to Loss of VHL Protein Expression Promotes the Malignancy Progression of Kidney Renal Clear Cell Carcinoma

Chenbin Cao[1,2,†], He Qi[1,2,†], Lu Xiang[2], Wenshuai Zhu[2], Yuxuan Shi[3], Xiaoli Ma[2], Yunshan Wang[2], Yanfei Jia[1,2], Yuanxin Xing[2,*]

[1]School of Medical Laboratory, Shandong Second Medical University, 261053 Weifang, Shandong, China
[2]Research Center of Basic Medicine, Central Hospital Affiliated to Shandong First Medical University, 250013 Jinan, Shandong, China
[3]Research Center of Basic Medicine, Jinan Central Hospital, Shandong University, 250013 Jinan, Shandong, China
*Correspondence: xyx15563369753@163.com (Yuanxin Xing)
[†]These authors contributed equally.

Academic Editor: Guoping Zheng
Submitted: 17 April 2026 Revised: 25 May 2026 Accepted: 28 May 2026 Published: 24 July 2026

Abstract

Background: Kidney renal clear cell carcinoma (KIRC) is the most common subtype of renal cell carcinoma, accounting for 75–80% of cases. Although Prohibitin 1 (*PHB1*) has been implicated in tumorigenesis, its role in KIRC remains unclear. This study aimed to investigate the expression, function, and underlying mechanisms of *PHB1* in KIRC. **Methods:** *PHB1* expression and clinical relevance were analyzed using the Cancer Genome Atlas database (TCGA), Gene Expression Omnibus database (GEO), and TIMER3.0 datasets. Single-cell RNA sequencing (scRNA-seq) data from 19 KIRC patients and normal kidney samples were used to assess cell-type-specific expression. Functional experiments, including CCK-8, EdU incorporation, colony formation, and Transwell assays, were performed to evaluate the effects of *PHB1* on cell proliferation, migration, and invasion. A xenograft model was used to evaluate the effects of *PHB1* in vivo. Western blotting and correlation analyses were conducted to assess the potential regulatory interplay between VHL, SKP2, PHB1, and p53. **Results:** *PHB1* was significantly downregulated in KIRC tissues. Single-cell analysis showed reduced *PHB1* expression in tumor-derived epithelial cells, fibroblasts, endothelial cells, and immune cells. Lower *PHB1* levels were associated with poorer overall survival. *PHB1* overexpression inhibited proliferation and migration, whereas knockdown promoted these effects. *In vivo*, *PHB1* overexpression reduced tumor growth. Moreover, VHL knockout altered the protein levels of SKP2 and *PHB1*. Cellular manipulation of *PHB1* moderately altered endogenous p53 protein expression. Based on TCGA data analysis, *PHB1* expression showed a positive correlation with VHL and a negative correlation with SKP2. **Conclusions:** Collectively, *PHB1* acts as a potential tumor suppressor in KIRC. Its expression pattern is associated with the VHL-SKP2 signaling axis, and the tumor-suppressive effects of *PHB1* may be partially associated with the modulation of p53 expression. These findings suggest that *PHB1* has the potential to serve as a reliable biomarker and therapeutic candidate for KIRC treatment.

Keywords: carcinoma; renal cell; *PHB1*; tumor microenvironment; biomarkers; prognosis

1. Introduction

Renal cell carcinoma (RCC) is one of the most common malignancies worldwide and primarily comprises three major subtypes, including kidney renal clear cell carcinoma (KIRC), chromophobe renal cell carcinoma (chRCC), and Papillary renal cell carcinoma (pRCC) [1,2,3,4]. Surgery remains the primary treatment method for localized tumors in KIRC, as this type of kidney cancer displays resistance to conventional radiotherapy and chemotherapy [5]. At present, nearly 30% of KIRC patients have distant metastasis at initial diagnosis [6]. The use of targeted treatment and immunotherapy has proven to improve the overall survival rate in patients with metastatic KIRC [7,8,9]. However, the presence of interindividual variability in treatment response and subsequent development of resistance in most patients results in a low 5-year survival rate of only 8% [4,10]. Consequently, a comprehensive understanding of the molecular mechanisms underlying KIRC progression and metastasis is essential for developing therapeutic strategies for advanced cases.

Prohibitin 1 (PHB1/PHB) is a ubiquitous protein that exists in numerous subcellular compartments of eukaryotic cells and is a member of the prohibitin protein family, which encompasses *PHB1* and *PHB2* [11]. These proteins can form high molecular weight complexes [12]. The complexes have been identified in mitochondria, plasma membrane, and nucleus [13]. Recent studies have reported upregulated *PHB1* expression in various human cancers, such as bladder cancer [14,15], lung cancer [16], breast cancer [17], ovarian cancer [18,19], melanoma [20] and prostate cancer [13]. For instance, increased levels of *PHB1* have been detected in human bladder cancer tissues, with predominant localization in mitochondria, and have been

strongly linked to a worsened prognosis for bladder cancer patients. *PHB1* is predominantly in the nucleus; however, treatment with camptothecin causes its translocation from the nucleus to the mitochondria as a reaction to apoptotic cues in breast cancer. Generally, the role of *PHB1* in various human cancers is intricately associated with specific cell types and their localization across different intracellular compartments. Nonetheless, several studies have shown *PHB1* as a tumor suppressor gene, including Human Liver Cancer [21,22] and nasopharyngeal carcinoma [23,24]. For example, LPLUNC1 is known to upregulate *PHB1* expression to inhibit the proliferation of nasopharyngeal carcinoma cells. Additionally, it has been observed that in human nasopharyngeal carcinoma tissue, the expression of *PHB1* is lower than in the adjacent normal tissues [25]. Nevertheless, the understanding of the expression and biological significance of *PHB1* in KIRC is limited.

This study conducted a pan-cancer analysis of *PHB1*, leveraging the comprehensive data from The Cancer Genome Atlas (TCGA) database. The findings uncovered that *PHB1* was highly expressed in most tumors, except for renal carcinoma and sarcoma. Notably, *PHB1* was most significantly downregulated in KIRC. Therefore, our findings contribute to elucidating the mechanisms of *PHB1* downregulation in KIRC and open new avenues for *PHB1*-based immunotherapy.

2. Materials and Methods

2.1 Bioinformatics Analysis

TIMER 3.0 (http://timer.cistrome.org/), GEO database (http://www.ncbi.nlm.nih.gov/geo) and Xiantao tool (https://www.xiantao.love/) were used to assess the differential expression of *PHB1* mRNA. The GEPIA 2.0 database (http://gepia2.cancer-pku.cn/) was used to explore the correlation between *PHB1* expression and overall survival (OS) as well as disease-free survival (DFS). Correlation analysis was performed using TIMER 3.0 and GEPIA 2.0. The CAMOIP (http://camoip.net/) and TCGA databases were analyzed to identify differentially expressed genes (DEGs) between patients with high and low *PHB1* expression (median value). Additionally, using TIMER 3.0, we analyzed the association between *PHB1* expression and tumor-infiltrating immune cells (TIICs), as well as between *PHB1* expression and immune-related genes in KIRC. The p-values reported by TIMER 3.0 were used as provided by the platform and were not adjusted for multiple comparisons (FDR correction was not applied).

2.2 Single-cell RNA-seq Data Mining

Data were retrieved from the GEO database, including scRNA-seq data of tumor tissues from 19 KIRC patients (GSE207493) and two normal renal tissue samples (GSE237425). Raw data were quantified via Cell Ranger (v6.1.2). The Seurat R package (v4.3.0) was used for quality control (200–5000 genes, <10% mitochondrial genes, >500 UMIs), normalization, dimensionality reduction, clustering and cell annotation. *PHB1* expression was visualized with bubble/dot/stacked bar plots. The Wilcoxon rank-sum test was used to compare *PHB1* expression between tumor and normal cells ($p < 0.05$).

2.3 Cell Culture and Reagents

Two RCC cell lines Caki-1 (TCHu135) and 786-O (TCHu186) were purchased from the Chinese Academy of Sciences (CAS) Cell Bank (Shanghai, China). All cell lines were authenticated by short tandem repeat (STR) profiling and confirmed to be free of mycoplasma contamination before use. Caki-1 cells were maintained in McCoy's 5A medium (Gibco, Cat. No. 16600082), while 786-O cells were cultured in RPMI-1640 medium (Gibco, Cat. No. 11875093). Both media were supplemented with 10% fetal bovine serum (Gibco, Cat. No. 10099141) and 1% penicillin-streptomycin (Gibco, Cat. No. 15140122). All cells were cultured at 37 °C in a humidified atmosphere with 5% CO_2. All transfections were conducted using the Lipo2000™ Transfection Reagent (Thermo Fisher Scientific, Cat# 11668019, Waltham, MA, USA) following the guidelines provided by the manufacturer.

2.4 Patient Samples

Tissue microarrays (TMAs) containing 75 pairs of KIRC tissues and matched adjacent non-tumor tissues were purchased from Shanghai Outdo Biotech Co., Ltd. (Shanghai, China; Cat. No. HKidCRCC150CS03). These samples were derived from patients with pathologically confirmed KIRC and were provided as commercially available tissue microarrays by Shanghai Outdo Biotech Co., Ltd.

2.5 Immunohistochemistry (IHC)

Immunohistochemistry (IHC) was performed based on previously described methods [26]. After deparaffinization, hydration, and antigen retrieval, the tissue sections were subjected to overnight incubation with primary antibodies (anti-PHB1, 1:300, Santa Cruz Biotechnology, Dallas, TX, USA, Cat# sc-3770375) at 4°C. The sections were then treated with the corresponding secondary antibody and observed using the DAB staining kit (Solarbio, Beijing, China, Cat# DA1010). Two independent pathologists, blinded to clinical data, evaluated staining intensity and percentage of positive cells.

2.6 Lentiviral Transduction and Establishment of Stable Cell Lines

The *PHB1* vector was prepared using the full-length complementary DNA (cDNA). Empty vector GV492 served as the control. Lentiviral vectors were cotransfected with psPAX2 and pMD2G into 293T cells to generate lentivirus. *PHB1* overexpression was achieved by transfecting the cells with the lentivirus. Stable clones were selected using puromycin (2 μg/mL, Sigma-Aldrich, St.

Louis, MO, USA, Cat# P9620) for a minimum of 1 week. The efficiency of overexpression was confirmed via Western blotting.

2.7 qRT-PCR

qRT-PCR was performed as previously described [27]. The utilized primer sequences included *GAPDH*: forward 5′-GCACCGTCAAGGCTGAGAAC-3′, reverse 5′-TGGTGAAGACGCCAGTGGA-3′, *PHB1*: forward 5′-TCATTTTCTCATCCCGTGGGTA-3′ reverse 5′-TGCCTGGAGACCAGCTCTCT-3′.

2.8 Western Blotting

The Western blotting procedure was carried out following the previously established methods [28]. The primary antibodies included: β-actin (1:3000; Abways, Shanghai, Shanghai, China, #CY1132), GAPDH (1:5000; Proteintech, Rosemont, IL, USA, #60004-1), PHB1 (1:1000; Santa Cruz Biotechnology, Dallas, TX, USA, #sc-3770375), PHB1 (1:1000; Servicebio, Wuhan, Hubei, China, #GB113098), E-cadherin (1:1000; Proteintech, Rosemont, IL, USA, #20874-1-AP), N-cadherin (1:1000; BD, Franklin Lakes, NJ, USA, #610920), SNAIL (1:1000; Proteintech, Rosemont, IL, USA, #13099-1-AP), Vimentin (1:1000; Proteintech, Rosemont, IL, USA, #10366-1-AP), SKP2 (1:1000; Cell Signaling Technology, Danvers, MA, USA, #2652), VHL (1:1000; Cell Signaling Technology, Danvers, MA, USA, #81292), p53 (1:1000; Proteintech, Rosemont, IL, USA, #10442-2-AP).

2.9 Plate Colony Formation Assay

Caki-1 (400 cells/well) and 786-O (400 cells/well) were seeded in separate wells of a 6-well plate. Two weeks after the initial seeding, the cells were fixed with 4% paraformaldehyde (Solarbio, Beijing, China, Cat# P1110) solution and stained with crystal violet solution (Solarbio, Beijing, China, Cat# IC0600).

2.10 Ethynyldeoxyuridine (EdU) Assays

The EDU assay was performed according to the manufacturer's protocol (RIBOBIO, Guangzhou, Guangdong, China, Cat# C10310-1), with results visualized under a microscope.

2.11 CCK-8 Assay

Cells from the Caki-1 line (3,000 cells per well) and the 786-O line (2,000 cells per well) were cultured in 96-well plates until they adhered to the wells. CCK-8 (Dojindo, Kumamoto, Japan, Cat# CK04) was dispensed into each well at time intervals of 0, 24, 48, 72, and 96 hours, followed by a 2-hour incubation at 37 ℃. The optical density was thereafter recorded at a wavelength of 450 nm to ascertain the absorbance levels.

2.12 Transwell Assay

Invasion and migration assessments were conducted using Transwell Chambers either lined with Matrigel or uncoated (Corning, Corning, NY, USA, Cat# 356234). The bottom compartment of the chambers was filled with Serum-containing medium. The upper compartment received seeding of Caki-1 and 786-O cells (10.0×10^4 cells) per well in a Serum-free medium. After a 24-hour incubation period, cells that had penetrated through the membrane were fixed in 4% paraformaldehyde and subsequently dyed with a crystal violet solution. Five random visual fields were assessed under a light microscope at 20× enlargement to quantify cells that traversed the membrane.

2.13 Immunofluorescence (IF)

FFPE TMA sections were deparaffinized, underwent antigen retrieval, and were permeabilized. After blocking with 10% goat serum, sections were incubated with primary antibodies (anti-PHB1, 1:200) overnight at 4°C, followed by Alexa Fluor secondary antibodies (1:500, 1 h, room temperature (RT)). The nucleus was stained with DAPI (Solarbio, Beijing, China, Cat# ID2250) before being observed under a Laser Confocal Microscope (TCS SP8, Leica, Germany).

2.14 CRISPR-Cas9-mediated Gene Disruption

VHL gene disruption was achieved using lentivirus-mediated CRISPR/Cas9 (JiKai Inc., Shanghai, China). A GV392 vector was used to incorporate a small guide RNA (sgRNA) specifically designed to target either human VHL or a non-target oligonucleotide. Briefly, 5×10^4 cells were infected at a MOI 10 in 250 µL culture medium with 1% FBS without antibiotics. After 12 hours, the medium was replaced by 500 µL culture medium + 10% FBS. Puromycin selection was used to enrich the lentivirus-infected cell populations. The two different nucleotide sequences used to target human VHL in this study included: (1) sgRNA1, 5′-AGTCAGAACCACAAACTGGT-3′ and (2) sgRNA2, 5′-ATGAGGTACTCACAAGCTCT-3′.

2.15 Tumor Xenografts

6-week-old male BALB/c nude mice were purchased from Beijing Vital River Laboratory Animal Technology Co., Ltd. (Beijing, China). Mice were randomly allocated to different experimental groups, and tumor measurement was performed in a blinded manner to avoid subjective bias. Exactly 6.0×10^6 Caki-1 cells were combined with Matrigel before being injected subcutaneously into the mice (n = 6/group). The tumor volume and body weight were measured and documented at two-day intervals. After 14 days, the mice were humanely euthanized by gradual displacement of carbon dioxide (CO_2) at a rate of 30–70% of the chamber volume per minute, and following the observation of respiratory arrest, the CO_2 flow was maintained for an additional 1 minute. The formula used to calculate

the tumor volume was: tumor volume = length × width^2 × 0.5. All animal experimental protocols were performed in line with the guidelines of the Ethics, Animal Care and Use Committee of Jinan Central Hospital (reference number JNCHIACUC2024-21).

All animal experiments were approved by the Ethics, Animal Care and Use Committee of Jinan Central Hospital (Approval No. JNCHIACUC2024-21) and conducted in accordance with the Guide for the Care and Use of Laboratory Animals and institutional guidelines for animal welfare. All animal experiments were conducted in accordance with the ARRIVE guidelines.

2.16 Statistical Analysis

Each *in vitro* experiment was performed with three independent biological replicates, and each biological replicate contained three technical replicates to ensure reproducibility. All data are presented as the mean ± SD. Statistical analyses were performed using Student's *t*-test or one-way ANOVA, as appropriate. Pearson correlation analysis was used to examine the correlation between *PHB1* expression and the clinicopathological characteristics of patients with KIRC. Significance was determined at $*p < 0.05$, $**p < 0.01$ and $***p < 0.001$.

3. Results

3.1 PHB1 Expression and Diagnostic Value in Pan-Cancer

A comprehensive analysis of the mRNA expression landscape of *PHB1* in human pan-cancer was conducted using the TIMER3.0 databases. *PHB1* expression was significantly upregulated in 12 cancer types. Moreover, KIRC had downregulated expression levels of *PHB1* compared to adjacent normal tissues (Fig. 1A, CHOL, COAD, BLCA, BRCA, LIHC, LUAD, ESCA, HNSC, STAD, UCEC, LUSC, READ, $p < 0.05$).

The relationship between *PHB1* levels and survival across multiple cancers was investigated using the GEPIA database. Consequently, we observed a relationship between downregulated *PHB1* expression and decreased OS in KIRC; on the other hand, lower *PHB1* levels corresponded with improved OS for BLCA, HNSC, LIHC, LGG, and LUAD (Fig. 1B). Furthermore, our findings revealed that upregulated *PHB1* expression was associated with improved DFS in KIRC patients, but poorer DFS in ACC, CESC, and PAAD (Fig. 1C). This suggests that *PHB1* may have significant biological relevance and potential implications in the context of KIRC, warranting further investigation.

3.2 PHB1 Was Correlated With Infiltrations of Immune Cells

KIRC is an immunogenic malignancy whose development is closely associated with the tumor immune microenvironment. We systematically analyzed the relationship between *PHB1* expression levels and the characteristics of the tumor immune microenvironment. Xiantao and TIMER3.0 database revealed that *PHB1* expression levels show significant correlations with the infiltration degrees of various immune cells, including $CD4^+$T cells, regulatory T cells (Tregs), immature dendritic cells (iDCs), and neutrophils (Fig. 2A–C). These results suggest that *PHB1* may influence the local immune landscape of KIRC by modulating the recruitment of specific immune subsets.

Given that the expression of immune checkpoint genes (ICGs) is a critical determinant of immunotherapy efficacy, we further utilized the TIMER 3.0 database to explore the association between *PHB1* expression and immune response-related checkpoint genes. The analysis indicated that several key immunosuppressive genes, including *LAG-3*, *TIGIT*, and *PDCD1* (*PD-1*) exhibit significant negative correlations with *PHB1* expression (Fig. 2D). Taken together, this study confirms that *PHB1* expression may influence the overall state of the tumor immune microenvironment in KIRC.

3.3 Single Cell Identification of Cell Types

To delineate the cell-type-specific expression pattern of PHB1 in normal and tumor tissues, we performed integrated single-cell RNA sequencing (scRNA-seq). Data quality was assessed using a Spearman correlation heatmap (Fig. 3A), which showed high inter-sample concordance and minimal batch effects. Unsupervised clustering via UMAP and t-SNE (Fig. 3B,C) identified eight major cell populations, including B cells, CAFs, endothelial cells, epithelial cells, mast cells, myeloid, NK cells and T cells, providing a comprehensive cellular atlas. To exclude confounding effects from cellular composition differences, we quantified the proportion of each cell type per sample (Fig. 3D); stacked bar plots revealed comparable distributions between normal and tumor tissues, suggesting that major differences are unlikely to be entirely explained by cell composition alone.

We then compared *PHB1* expression across these annotated cell types between normal and tumor samples (Fig. 3E). Violin plots displayed a distinct cell-type-specific pattern: *PHB1* was significantly downregulated in tumor-derived epithelial cells, fibroblasts, endothelial cells, B cells, myeloid cells, and T cells. In contrast, mast cells exhibited higher *PHB1* expression. These results were further supported by a dot plot (Fig. 3F), summarizing both average expression and the percentage of *PHB1*-positive cells across all types, consistently indicating broad *PHB1* downregulation in most tumor-associated cellular compartments.

3.4 Clinical Significance and Prognostic Value of PHB1 in KIRC

Subsequently, we investigated the expression of *PHB1* in KIRC. GEPIA2 and Xiantao database analyses demonstrated that *PHB1* was downregulated in KIRC tissues compared to matched normal tissues (Fig. 4A). This conclusion was further confirmed by GEO data analysis (Fig. 4B).

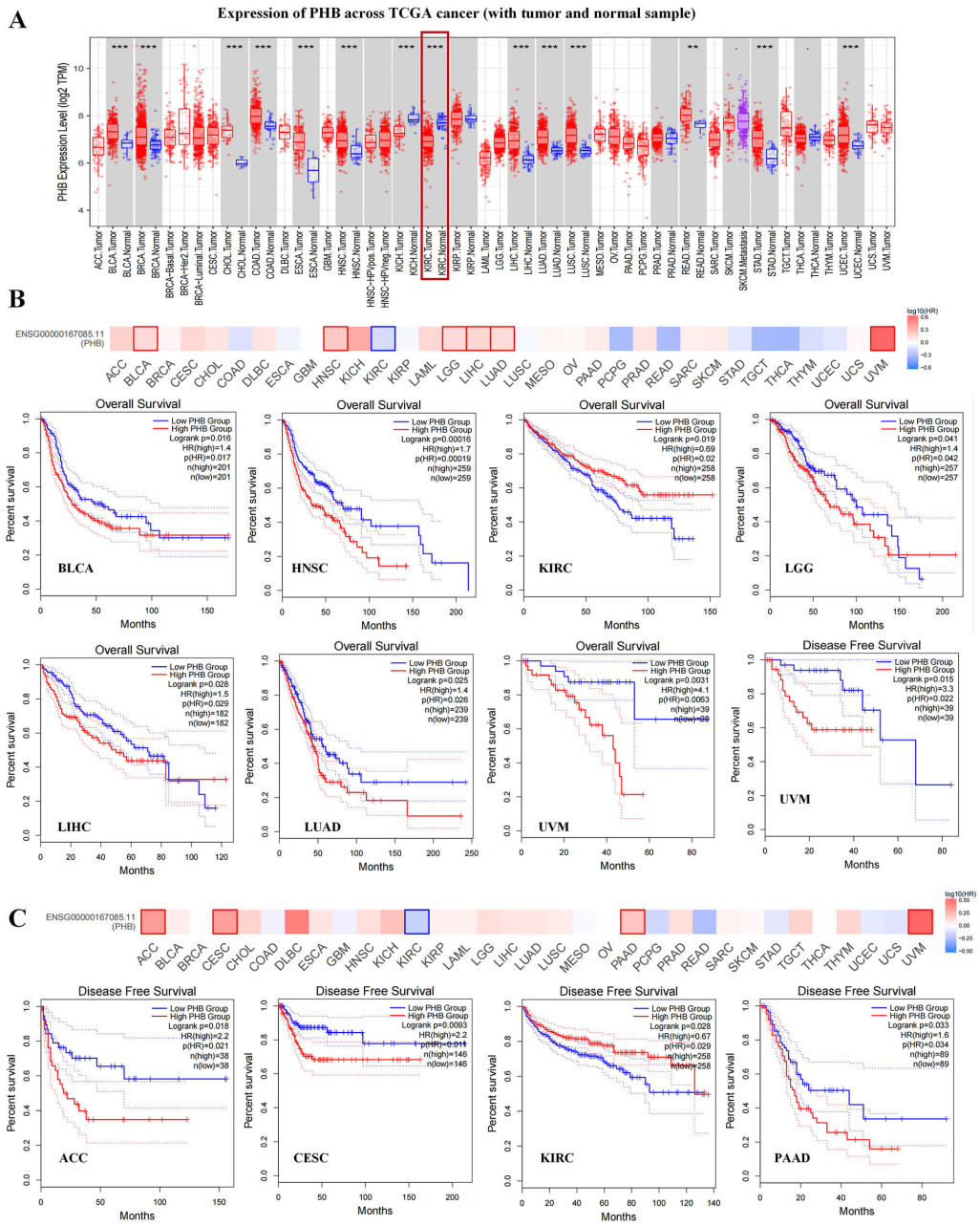

Fig. 1. *PHB1*expression in pan-cancer from different databases Survival analysis of *PHB1* in different types of cancer. (A) Using the TIMER3.0 databases to analyze the expression levels of *PHB1* mRNA in human pan-cancer (ACC, adrenocortical carcinoma; BLCA, bladder urothelial carcinoma; BRCA, breast invasive carcinoma; CESC, cervical squamous cell carcinoma; CHOL, cholangiocarcinoma; COAD, colon adenocarcinoma; DLBC, diffuse large B-cell lymphoma; ESCA, esophageal carcinoma; GBM, glioblastoma multiforme; HNSC, head and neck squamous cell carcinoma; KICH, kidney chromophobe; KIRC, kidney renal clear cell carcinoma; KIRP, kidney renal papillary cell carcinoma; LAML, acute myeloid leukemia; LGG, low-grade glioma; LIHC, liver hepatocellular carcinoma; LUAD, lung adenocarcinoma; LUSC, lung squamous cell carcinoma; MESO, mesothelioma; OV, ovarian serous cystadenocarcinoma; PAAD, pancreatic adenocarcinoma; PCPG, pheochromocytoma and paraganglioma; PRAD, prostate adenocarcinoma; READ, rectum adenocarcinoma; SARC, sarcoma; SKCM, skin cutaneous melanoma; STAD, stomach adenocarcinoma; TGCT, testicular germ cell tumor; THCA, thyroid carcinoma; THYM, thymoma; UCEC, uterine corpus endometrial carcinoma; UCS, uterine carcinosarcoma; UVM, uveal melanoma. Blue color indicates normal tissues; red color indicates tumor tissues). (B,C) Using the GEPIA database to analyze the correlation of Prohibitin 1 (*PHB1*) expression with overall survival (OS) (B) and disease-free survival (DFS) (C) in patients with different cancers. TCGA, The Cancer Genome Atlas. $^{**}p < 0.01$, $^{***}p < 0.001$.

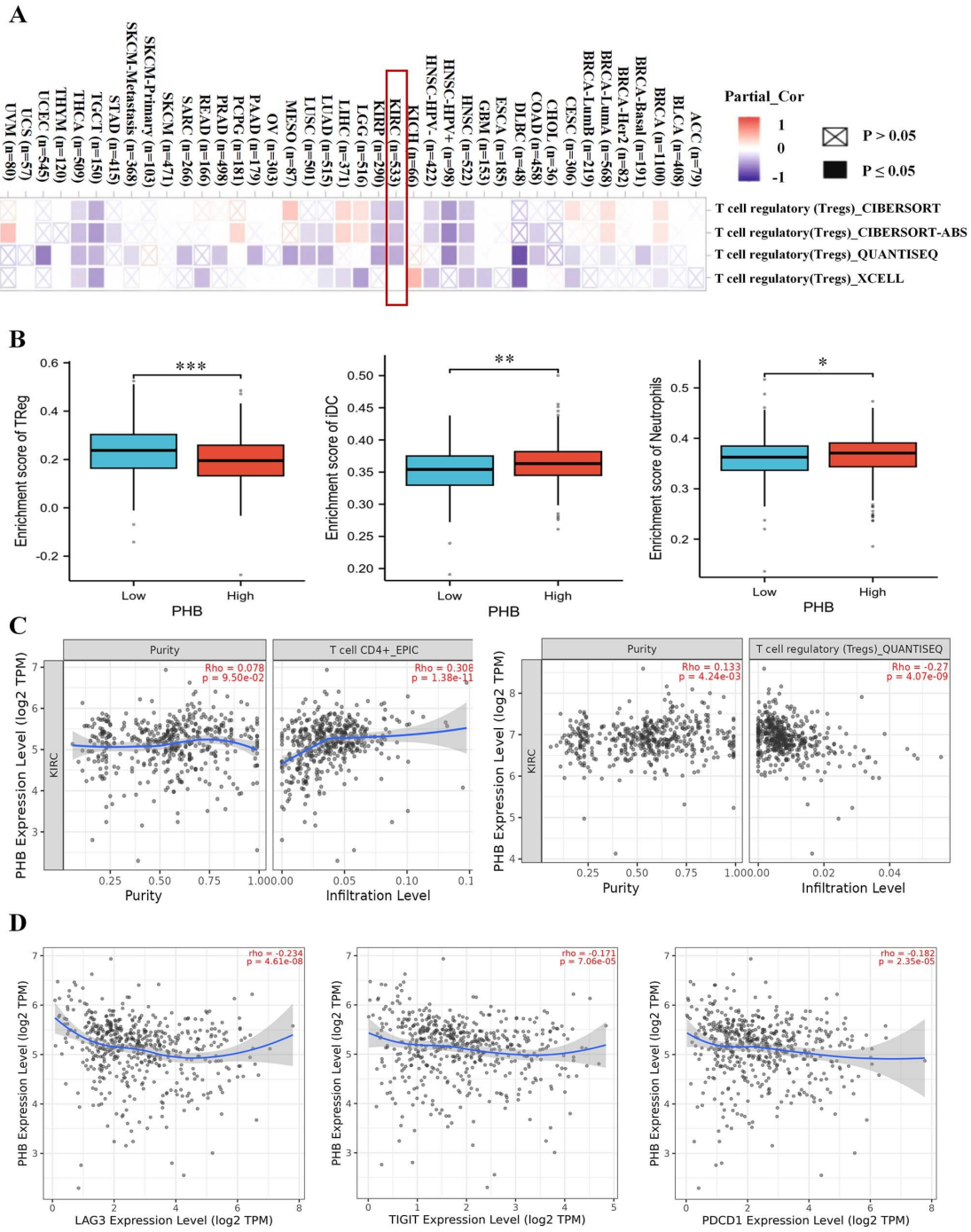

Fig. 2. Correlation between *PHB1* expression and immune infiltration in KIRC. (A) Correlations between *PHB1* expression and infiltration of immune cells. (B) Box plots comparing the infiltration levels of regulatory T cells (Tregs), immature dendritic cells (iDCs), and neutrophils between high and low *PHB1* expression groups. (C) Scatter plot depicting the correlation between *PHB1* expression and CD4+T cell, Tregs cells level. (D) Correlation of *PHB1* with the immune checkpoint. *$p < 0.05$, **$p < 0.01$, ***$p < 0.001$.

In addition, we analyzed the association between *PHB1* expression and clinicopathological characteristics using the Xiantao database. The results showed that patients with greater depth of invasion and more advanced tumor stage tended to exhibit lower *PHB1* expression levels in primary tumors (Fig. 4C and Table 1). A total of 523 patients with KIRC from the TCGA database were included in the prognostic analysis. Multivariate Cox regression analysis demonstrated that *PHB1* expression remained significantly associated with overall survival after adjustment for age, gender, tumor grade, and pathological stage (hazard ratio [HR] = 1.434, 95% confidence interval [CI]: 1.056–

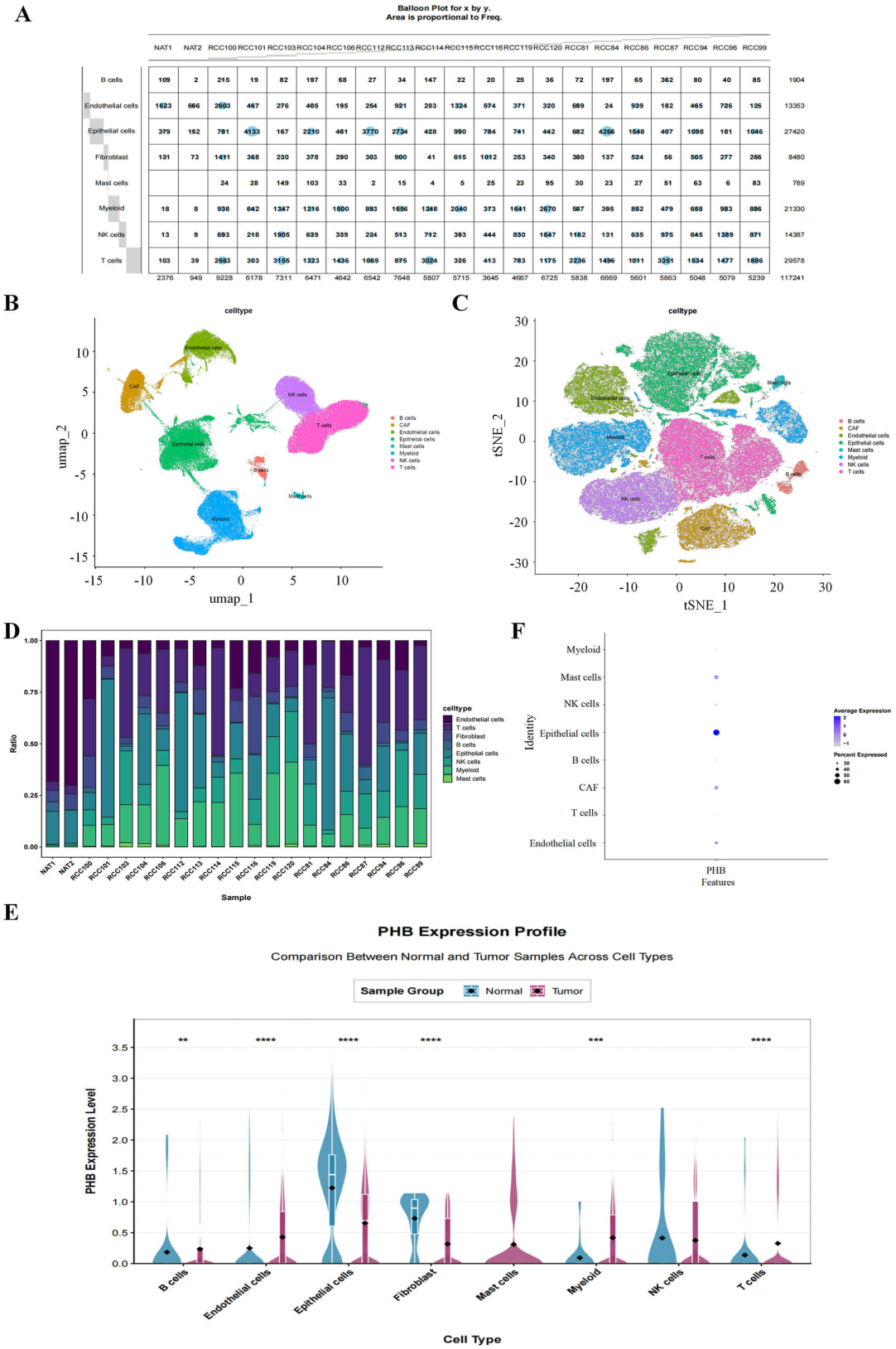

Fig. 3. Single-cell landscape of *PHB1*expression in normal and KIRC tissues. (A) Spearman correlation heatmap showing inter-sample concordance and minimal batch effects. (B,C) Unsupervised clustering visualized by UMAP (B) and t-SNE (C), identifying eight major cell populations. (D) Stacked bar plot showing the proportion of each cell type in normal versus tumor samples. (E) Violin plots comparing *PHB1* expression across cell types between normal and tumor tissues. (F) Dot plot summarizing the average expression level and the percentage of *PHB1*-positive cells for each cell type. $^{**}p < 0.01$, $^{***}p < 0.001$, $^{****}p < 0.0001$.

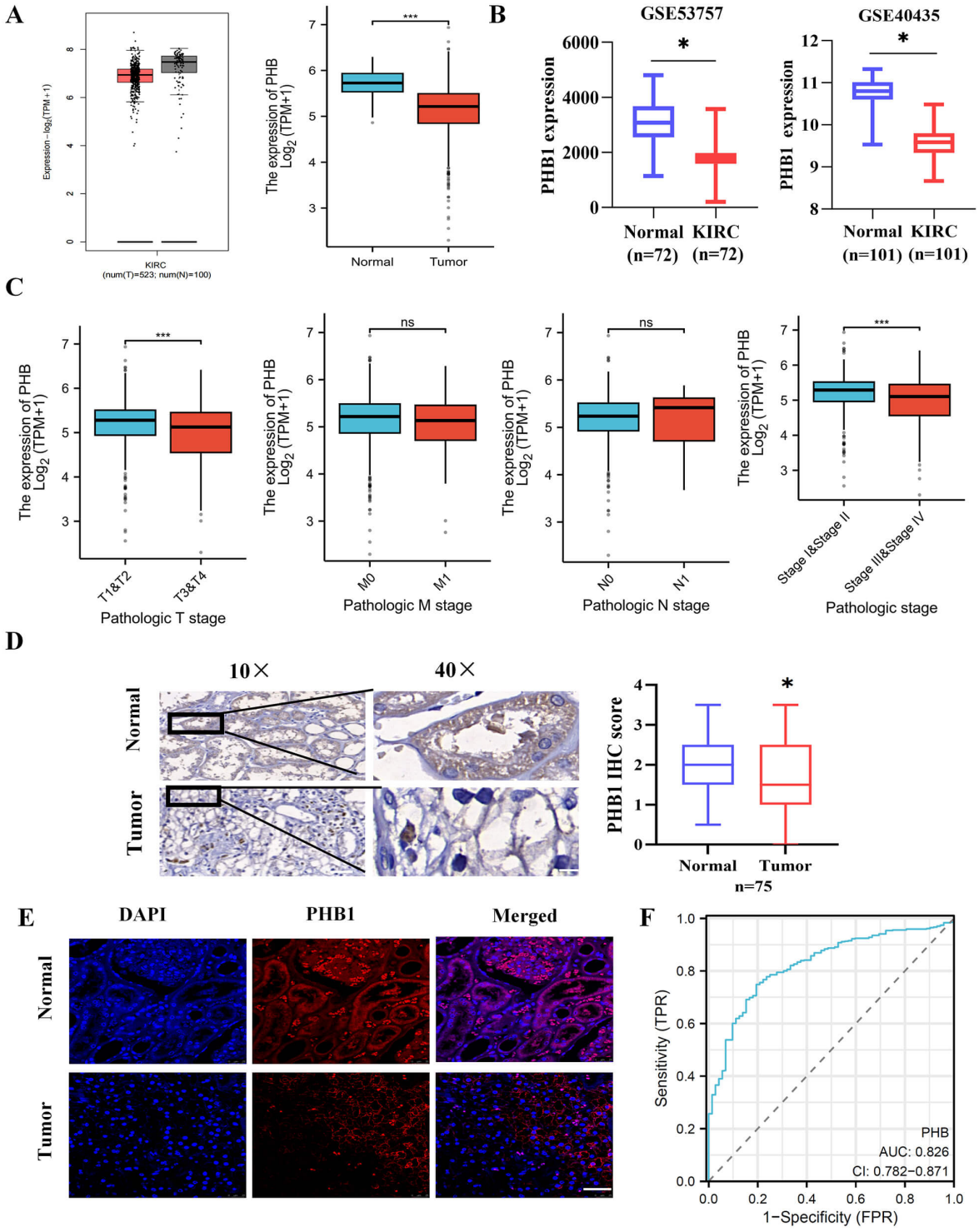

Fig. 4. *PHB1* is down-regulated in clinical sample. (A) Analysis of *PHB1* expression in GEPIA2 (left) and Xiantao (right) database. (B) Analysis of *PHB1* expression in datasets of GSE53757 (left) and GSE40435 (right). (C) Correlation between *PHB1* expression and clinicopathological features. (D) *PHB1* IHC staining of TMA. Scale bars: 100 μm (original image) and 20 μm (enlarged view). (E) *PHB1* IF staining of TMA. Scale bars: 100 μm. (F) Diagnostic value of *PHB1* in KIRC, as determined by ROC curve analysis. IHC, Immunohistochemistry; IF, Immunofluorescence; FPR, false positive rate; TPR, true positive rate; ROC, receiver operating characteristic; ns, not significant; *$p < 0.05$, ***$p < 0.001$.

Table 1. Association of *PHB1* expression with clinicopathological characteristics of patients with KIRC.

Characteristic (n = 75)	High expression of *PHB1*	Low expression of *PHB1*	*p* value
Gender			0.126
Male	15	35	
Female	12	13	
Age (years)			0.307
≤60	20	30	
>60	7	18	
T stage			**0.015***
T1–T2	24	30	
T3–T4	3	18	
N stage			0.360
N0	26	48	
N1	1	0	
M stage			1.000
M0	26	47	
M1	1	1	

Bold indicates a statistically significant value. *$p < 0.05$.

Table 2. Multivariate cox regression analysis of overall survival in patients with KIRC.

Variables (n = 523)	*p* value	HR	Multivariate HR (95% CI)
Age	<0.001	1.026	1.012–1.041
Gender	0.562	0.908	0.656–1.257
Grade	<0.001	1.898	1.325–2.719
Stage	<0.001	3.126	2.238–4.367
PHB1	0.021	1.434	1.056–1.947

1.947, $p = 0.021$), suggesting that *PHB1* may serve as an independent prognostic factor in KIRC (Table 2). Subsequent IHC and IF analyses of a TMA containing 75 paired KIRC and adjacent normal specimens demonstrated significant downregulation of *PHB1* expression in tumor tissues (Fig. 4D,E). ROC curve analysis demonstrated that *PHB1* exhibited high diagnostic value for KIRC, with an AUC of 0.826 (Fig. 4F). These findings support a potential role of *PHB1* in KIRC progression.

3.5 PHB1 Inhibits KIRC Cell Proliferation In Vitro *and Tumor Formation* In Vivo

Gain and loss-of-function analyses were conducted in 786-O and Caki-1 cells to investigate the impact of *PHB1* on KIRC progression. *PHB1*-specific siRNA was used to knockdown *PHB1* expression in 786-O cells. Caki-1 cells were infected with *PHB1*-expressing lentivirus and control lentivirus to construct *PHB1* overexpression stable cell line (*PHB1*) and control stable cell line (Vector) (Fig. 5A). We used colony formation assays (Fig. 5B), EdU assay (Fig. 5C) and CCK-8 assay (Fig. 5D) to quantify cell growth and found that *PHB1* downregulation markedly increased cell proliferation, whereas *PHB1* overexpression significantly suppressed cell growth. The results showed that *PHB1* may play an important role in KIRC progression.

To further investigate the role of *PHB1* in KIRC growth and development *in vivo*, a 6-week-old nude mouse xenograft model was employed. Caki-1 cells, either *PHB1* or Vector, were subcutaneously injected into the mice. Tumor growth assessments revealed that *PHB1* overexpression significantly reduced both average tumor volume and weight compared to EV (Fig. 5E,F). In summary, *PHB1* overexpression inhibited KIRC growth *in vivo*.

3.6 PHB1 Inhibits KIRC Cell Migration In Vitro

We further observed that *PHB1* overexpression remarkably suppressed the migration and invasion capacities of Caki-1 cells. Conversely, *PHB1* knockdown in 786-O cells had the opposite effect (Fig. 6A).

The capacity of tumors to migrate is underpinned by epithelial-mesenchymal transition (EMT). Pearson correlation analysis revealed that *PHB1* expression was negatively correlated with mesenchymal markers (Snail, N-cadherin) and positively correlated with epithelial markers (E-cadherin) (Fig. 6B). Western blotting results revealed that *PHB1* overexpression upregulated E-cadherin expression while also downregulating N-cadherin, Snail and Vimentin expression. In contrast, *PHB1* knockdown downregulated the expression levels of E-cadherin and upregulated the protein levels of N-cadherin, Snail, and Vimentin (Fig. 6C). Collectively, these results indicate that *PHB1* inhibits the migration of KIRC cells.

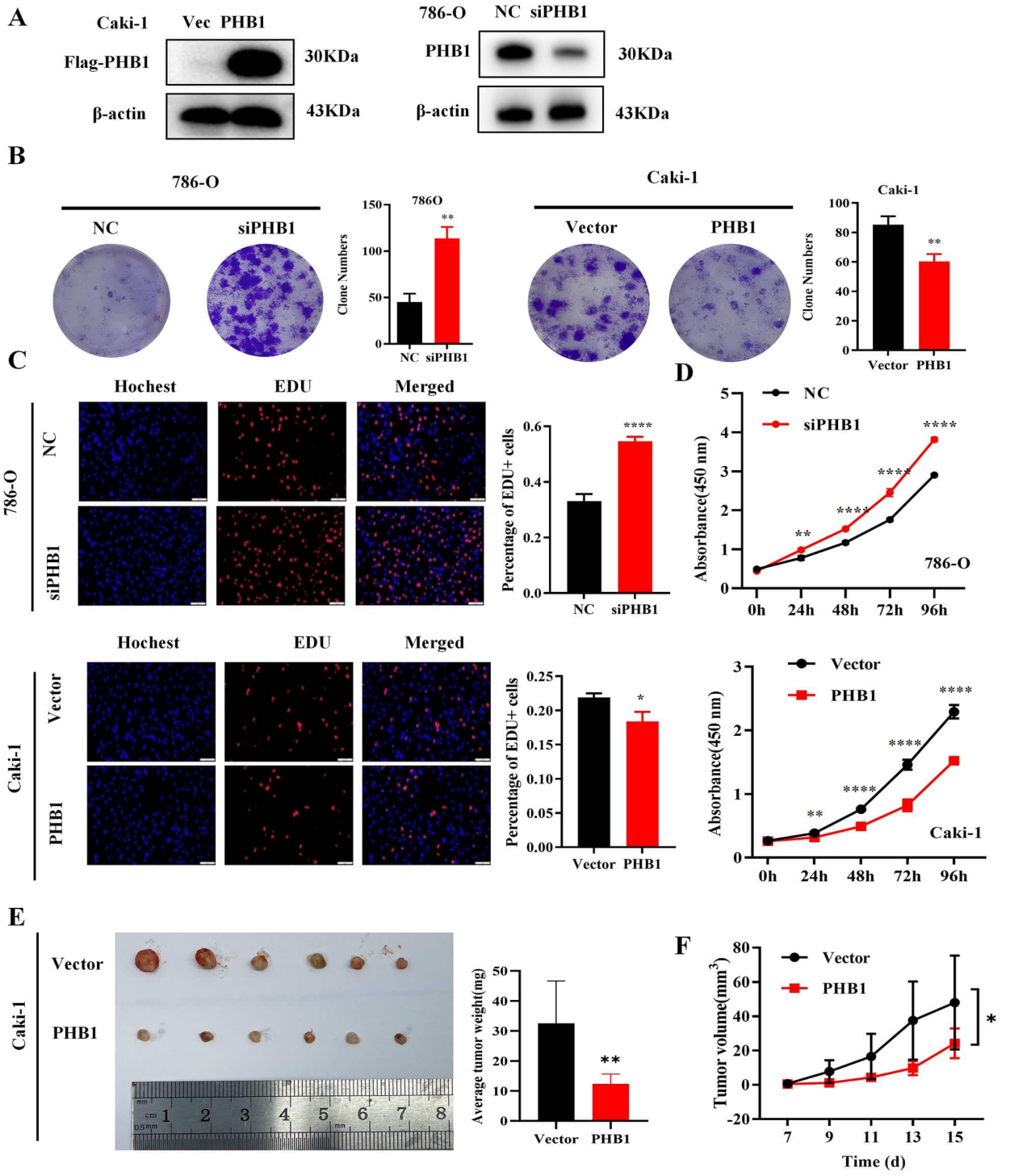

Fig. 5. *PHB1* inhibits KIRC cell proliferation *in vitro* and tumor formation *in vivo*. (A) Western blot validation of *PHB1* knockdown in 786-O cells and overexpression in Caki-1 cells. (B) Plate colony formation assays and quantitative analysis. (C) EdU test and quantitative analysis. Scale bar = 100 μm. (D) The results of CCK-8 assays. (E,F) High expression of *PHB1* inhibits tumorigenesis in nude mice. NC, negative control. *$p < 0.05$, **$p < 0.01$, ****$p < 0.0001$.

3.7 VHL/SKP2/PHB1/p53 Axis-regulated KIRC Progression

Next, the mechanisms underlying low *PHB1* expression in KIRC were further investigated. The correlation analysis from the GEPIA database suggested that *PHB1* expression was significantly positively correlated with VHL expression (Fig. 7A). Studies have shown that, pVHL interacts with SKP2, hence stimulating proteasome-dependent

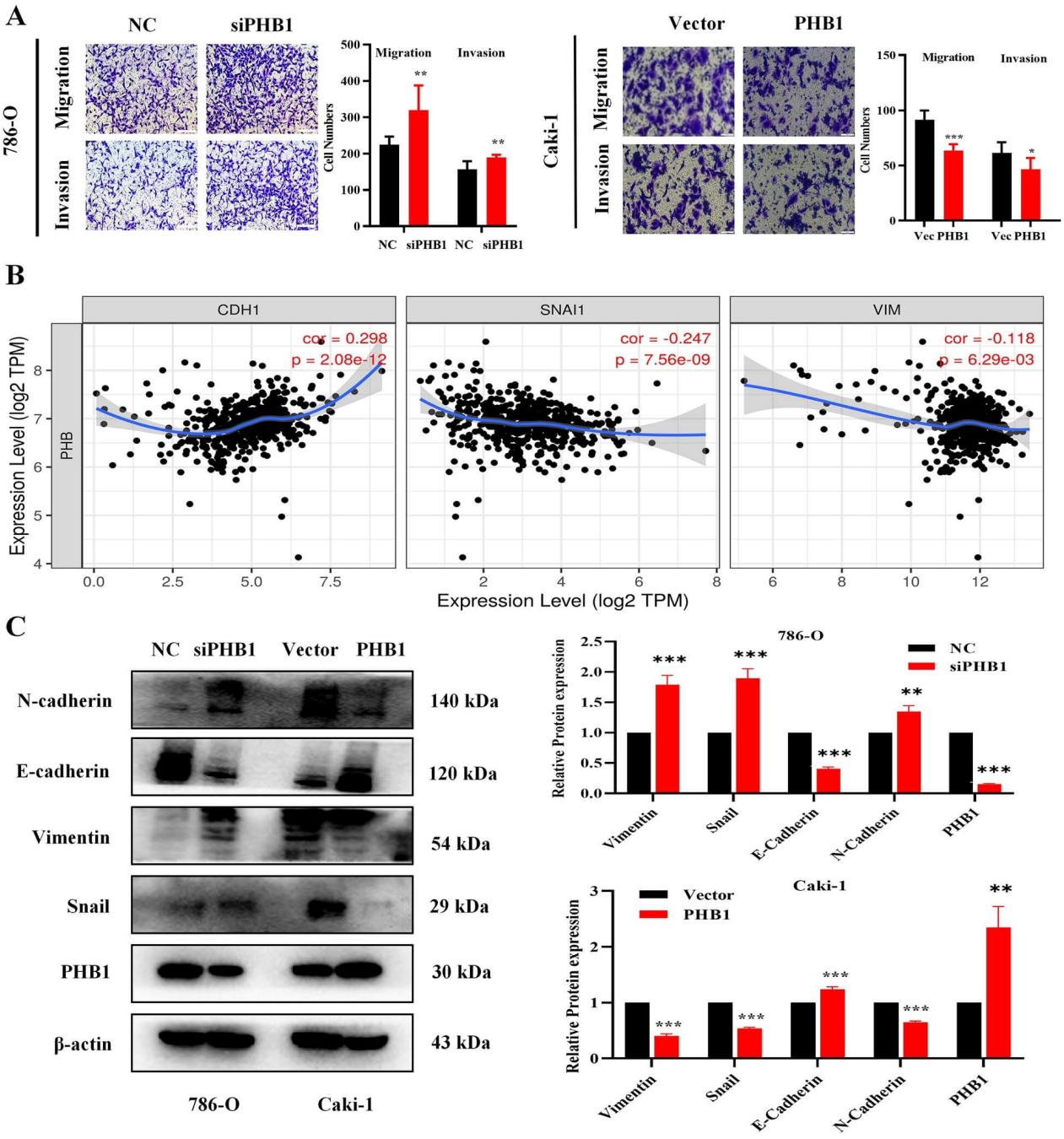

Fig. 6. *PHB1*inhibits KIRC cell migration *in vitro*. (A) Migration/invasion assays and quantitative analysis. For each experimental trial, cells were enumerated in 5 randomly selected fields on each filter using a microscope with a 20× magnification. Scale bar = 100 μm. (B) A Pearson correlation analysis of *PHB1* and EMT markers (E-cadherin, Snail, Vimentin) in KIRC using the TIMER3.0 database. (C) Analysis of protein expression of E-cadherin, N-cadherin, Vimentin, and Snail in 786-O and Caki-1 cells with knockout or ectopic expression of *PHB1* by Western blot. *$p < 0.05$, **$p < 0.01$, ***$p < 0.001$.

degradation of SKP2 [29]. Meanwhile, *PHB1* is a substrate of SKP2 in breast cancer [30]. Based on these findings, we hypothesized that VHL may regulate *PHB1* stability through the SKP2-mediated ubiquitin–proteasome pathway. Western blot analysis revealed that *PHB1* expression was markedly reduced, whereas SKP2 expression was increased, in VHL-deficient 786-O ($VHL^{-/-}$) cells compared with Caki-1 ($VHL^{+/+}$) cells (Fig. 7B). Subsequently, CRISPR-Cas9-mediated genome editing technology was used to generate Caki-1 Cas9 CRISPR KO VHL (KO VHL, KO) and Caki-1-Cas9 (Wildtype VHL, WT) cells. As shown in Fig. 7C, VHL knockout significantly downreg-

ulated *PHB1* expression while simultaneously upregulating SKP2 expression in Caki-1 cells (Fig. 7C). Furthermore, ubiquitination assays demonstrated that VHL knockout markedly increased *PHB1* ubiquitination levels, and this effect was further enhanced following treatment with the proteasome inhibitor MG132 (Fig. 7D). These findings suggest that VHL loss may contribute to *PHB1* downregulation by increasing SKP2 expression and promoting ubiquitin–proteasome-dependent degradation of *PHB1*.

To further elucidate the mechanisms by which *PHB1* functions in KIRC, Gene Set Enrichment Analysis (GSEA) was performed using the CAMOIP database. The results revealed a strong association between *PHB1* expression and the p53 signaling pathway (Fig. 7E). In addition, the STRING database was used to explore the molecular interactions and functional pathways associated with the candidate genes (Fig. 7F). Previous studies have reported that *PHB1* can physically interact with p53 and enhance p53-mediated transcriptional activity [31]. Therefore, we speculated that *PHB1* may suppress KIRC progression, at least in part, by modulating the p53 signaling pathway. Consistently, correlation analysis showed that *PHB1* was closely associated with p53 expression in KIRC (Fig. 7G). Western blot analysis further demonstrated that *PHB1* knockdown reduced p53 protein expression, whereas ectopic *PHB1* expression increased p53 protein levels in KIRC cells (Fig. 7H). Taken together, these findings suggest that *PHB1* may inhibit KIRC progression, at least partially, through regulation of p53 expression.

4. Discussion

The *PHB1* gene was first isolated and characterized as a potential anti-proliferation gene in rat liver cells [32]. Several research reports have shown that *PHB1* is a potential target for cancer therapy [33]. Nonetheless, the expression patterns and roles of *PHB1* in the progression of renal carcinoma remain elusive. Herein, a pan-cancer analysis of *PHB1* was performed based on a comprehensive examination of TCGA. Notably, *PHB1* is highly expressed in most of the tumors, except renal carcinoma and sarcoma. Additional evidence indicates that *PHB1* is significantly downregulated in KIRC, unlike in sarcoma and KICH. Therefore, the present study investigated the expression status and roles of *PHB1* in the progression of KIRC. It was observed that *PHB1* was significantly downregulated in KIRC. Low *PHB1* expression was associated with poor prognosis. Functional studies showed that *PHB1* overexpression suppressed cell proliferation and migration, and promoted autophagy. *PHB1* knockdown exhibited the opposite effects. Our findings suggest that *PHB1* may play an important anti-cancer role in KIRC.

KIRC is increasingly recognized as a metabolic disease characterized by extensive reprogramming of energy metabolism, including enhanced glycolysis, impaired mitochondrial oxidative phosphorylation (OXPHOS), and abnormal lipid metabolism [34,35]. These metabolic alterations not only promote tumor progression, but also influence drug sensitivity and the maintenance of cancer stem cell properties. *PHB1* is an important regulator of mitochondrial function and cellular energy metabolism, and accumulating evidence suggests that *PHB1* plays a critical role in maintaining mitochondrial homeostasis and regulating metabolic processes in cancer cells [36,37]. Therefore, investigating the biological role of *PHB1* in KIRC is of particular significance, as it may provide new insights into the metabolic mechanisms underlying KIRC progression and identify potential therapeutic targets related to mitochondrial energy metabolism.

In further analyses, we investigated the factors driving the low *PHB1* expression. It has been reported that the short arm of chromosome 3 is lost in approximately 90% of KIRC [38]. The missing region encodes the tumor suppressor gene VHL, a 24 kDa protein with several roles [39,40]. We further investigated whether *PHB1* and VHL protein levels were related. Interestingly, the correlation analysis revealed a substantial positive relationship between *PHB1* expression and VHL expression. Moreover, Western blotting showed that VHL promotes *PHB1* expression. Reports indicate that pVHL interacts with SKP2, causing proteasome-dependent SKP2 degradation. Moreover, one study has shown that *PHB1* is a substrate of SKP2 in breast cancer cells [30]. Therefore, we hypothesized that the low expression of *PHB1* may be attributed to the pVHL deletion, which may increase SKP2 expression and thereby promote proteasome-dependent degradation of *PHB1*. The Western blotting results were consistent with this hypothesis.

Previous reports have shown that *PHB1* exerts anticancer effects by interacting with various transcription factors, including p53, c-myc, Rb, and E2F [11,41,42,43,44]. Fusaro et al. [31] revealed that *PHB1* improves p53-mediated transcriptional activity. Therefore, we speculate that *PHB1* suppresses cancer progression by regulating p53 expression. The correlation analysis revealed that *PHB1* expression is significantly positive with p53 expression. Additionally, Western blotting results demonstrated that *PHB1* knockdown down-regulates p53 protein expression. Conversely, ectopic *PHB1* expression upregulated p53 protein expression in KIRC cells. As such, our findings suggest that *PHB1* may serve as a tumor suppressor in KIRC, partially through modulating the p53 signaling pathway.

In addition, KIRC is considered one of the most immune-infiltrated tumor types, and increasing evidence suggests that metabolic reprogramming is closely associated with angiogenesis, inflammatory signaling, and immune cell infiltration in the tumor microenvironment [45]. Since the tumor microenvironment plays an important role in disease progression and therapeutic response, these metabolic and immune characteristics may together influ-

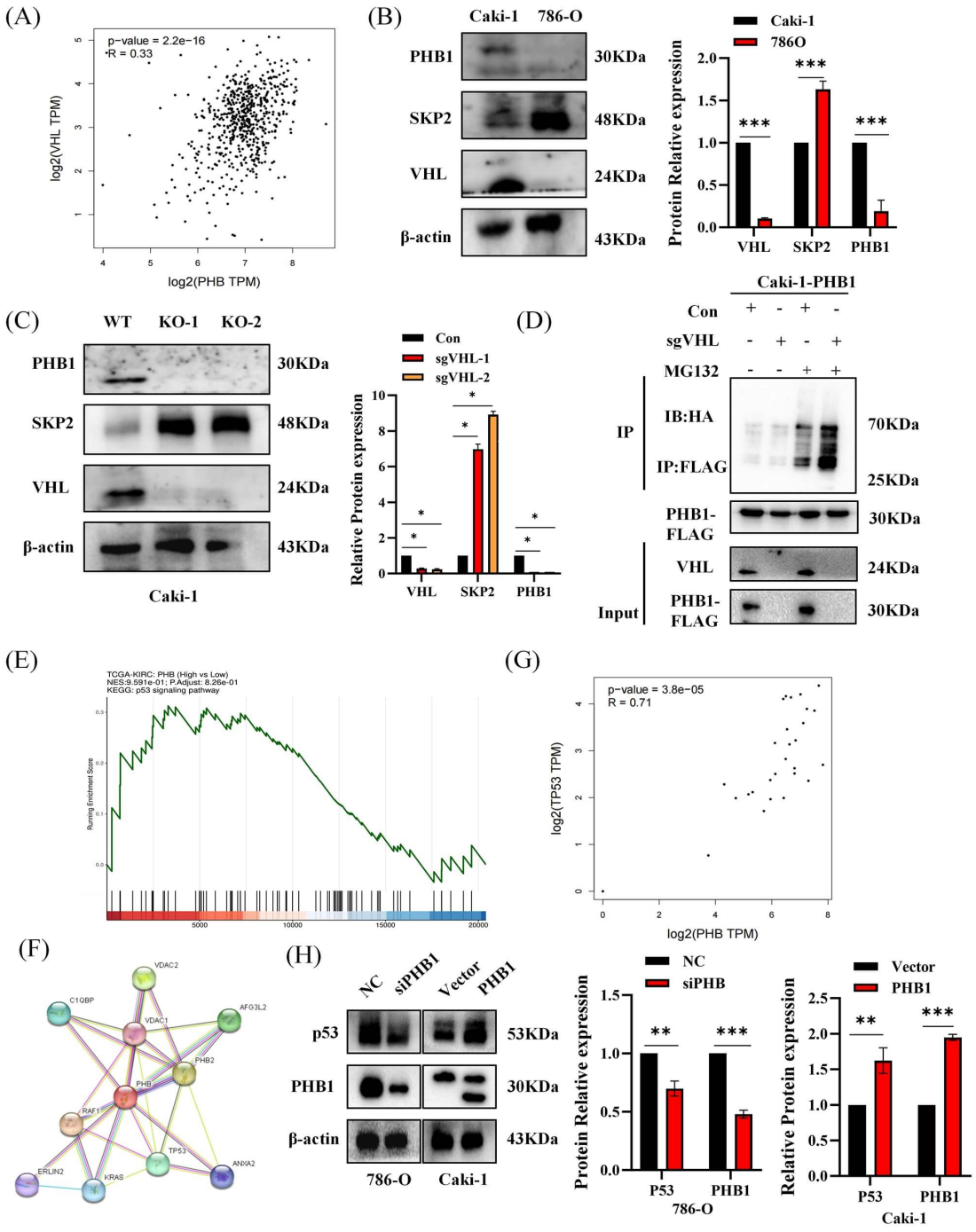

Fig. 7. *VHL/SKP2/PHB1/p53* axis-regulated KIRC progression. (A) The GEPIA database was used to analyze the correlation between *PHB1* and VHL expression in KIRC patients. (B) The protein expression of VHL, SKP2, and *PHB1* in 786-O and Caki-1 cells was analyzed by Western blot, n = 3. (C) The protein expression of VHL, SKP2, and *PHB1* in Caki-1(KO VHL) and Caki-1 (WT VHL) cells was assayed by Western blot, n = 3. (D) *PHB1*-FLAG was immunoprecipitated and analyzed by immunoblotting with anti-ubiquitin antibodies in the presence or absence of MG132 in VHL-deficient and control cells. (E) GSEA reveals a significant correlation between elevated *PHB1* expression and the p53 signaling pathway. (F) The available experimentally determined *PHB1* binding proteins were obtained using the STRING database. (G) The correlation between *PHB1* and *TP53* expression in KIRC patients was assessed using the GEPIA database. (H) Western blot analysis for protein expression of p53 in 786-O and Caki-1 cells with ectopic or knockout expression of *PHB1*, n = 3. **p* < 0.05, ***p* < 0.01, ****p* < 0.001.

ence the efficacy of systemic therapies in KIRC. Previous studies have also indicated that *PHB1* is involved in the regulation of mitochondrial homeostasis and inflammatory responses and may participate in immune-related biological processes [36]. Therefore, *PHB1* may contribute to the regulation of the immune microenvironment in KIRC, although the underlying mechanisms require further investigation.

Limitations

Notably, although we observed a correlation between *PHB1* and p53 expression, we have not conducted rescue experiments to validate whether p53 is an essential functional mediator of *PHB1*. Given these limitations, as well as the relatively limited sample size of our protein expression cohort, further comprehensive investigations, especially *in vivo* functional validation, are required to precisely clarify the direct downstream molecular targets of *PHB1*.

5. Conclusions

In conclusion, we found that *PHB1* may act as a tumor suppressor in KIRC. Besides, its low expression is attributed to SKP2 upregulation caused by VHL deletion or reduction, hence promoting ubiquitination and degradation of *PHB1*. More importantly, *PHB1* might be a tumor suppressor through the p53 pathway. These findings provide novel perspectives on the molecular mechanism of KIRC, indicating that *PHB1* is a potential treatment target for KIRC patients.

Abbreviations

Cas9, CRISPR associated protein 9; CRISPR, Clustered Regularly Interspaced Short Palindromic Repeats; EMT, epithelial-mesenchymal transition; GEO, Gene Expression Omnibus database; KIRC, kidney renal clear cell carcinoma; PHB1, prohibitin 1; TCGA, The Cancer Genome Atlas database.

Availability of Data and Materials

All the data will be available upon request.

Author Contributions

CC: Methodology, Investigation. HQ: Methodology, Investigation. LX: Methodology, Investigation. WZ: Methodology, Investigation. YS: Investigation, Writing - original draft. XM: Writing - original draft, Data curation. YW: Writing - review & editing, Conceptualization. YJ: Writing - original draft. Writing - original draft, Data curation. YX: Writing - review & editing, Conceptualization. All authors contributed to critical revision of the manuscript for important intellectual content. All authors reviewed and approved the final manuscript. All authors have participated sufficiently in the work and agreed to be accountable for all aspects of the work.

Ethics Approval and Consent to Participate

All animal experiments were approved by the Ethics, Animal Care and Use Committee of Jinan Central Hospital (Approval No. JNCHIACUC2024-21) and conducted in accordance with the Guide for the Care and Use of Laboratory Animals and institutional guidelines for animal welfare. All animal experiments were conducted in accordance with the ARRIVE guidelines.

Acknowledgment

We thank the TCGA, GEO and other databases for providing invaluable data for statistical analyses.

Funding

This work was supported by the Jinan Municipal Health Commission Science and Technology Program (No. 2023-1-5).

Conflicts of Interest

The authors declare no conflicts of interest.

Supplementary Material

Supplementary material associated with this article can be found, in the online version, at https://doi.org/10.31083/FBL53057.

References

[1] Hsieh JJ, Purdue MP, Signoretti S, Swanton C, Albiges L, Schmidinger M, et al. Renal cell carcinoma. Nature Reviews. Disease Primers. 2017; 3: 17009. https://doi.org/10.1038/nrdp.2017.9

[2] Siegel RL, Miller KD, Wagle NS, Jemal A. Cancer statistics, 2023. CA: a Cancer Journal for Clinicians. 2023; 73: 17–48. https://doi.org/10.3322/caac.21763

[3] Ricketts CJ, De Cubas AA, Fan H, Smith CC, Lang M, Reznik E, et al. The Cancer Genome Atlas Comprehensive Molecular Characterization of Renal Cell Carcinoma. Cell Reports. 2018; 23: 313–326.e5. https://doi.org/10.1016/j.celrep.2018.03.075

[4] Rini BI, Campbell SC, Escudier B. Renal cell carcinoma. Lancet (London, England). 2009; 373: 1119–1132. https://doi.org/10.1016/S0140-6736(09)60229-4

[5] Thomas JS, Kabbinavar F. Metastatic clear cell renal cell carcinoma: A review of current therapies and novel immunotherapies. Critical Reviews in Oncology/hematology. 2015; 96: 527–533. https://doi.org/10.1016/j.critrevonc.2015.07.009

[6] Chen X, Liu Y, Wang T, Liu D, Chang P, Liu N, et al. Development and validation of a diagnostic nomogram integrating anatomical scores and systemic immune-inflammatory biomarkers for De Novo metastatic renal cell carcinoma: a single-center, retrospective study (2016-2025). Frontiers in Immunology. 2026; 17: 1747057. https://doi.org/10.3389/fimmu.2026.1747057

[7] Ballesteros PÁ, Chamorro J, Román-Gil MS, Pozas J, Gómez Dos Santos V, Granados ÁR, et al. Molecular Mechanisms of Resistance to Immunotherapy and Antiangiogenic Treatments in Clear Cell Renal Cell Carcinoma. Cancers. 2021; 13: 5981. https://doi.org/10.3390/cancers13235981

[8] Kim MC, Jin Z, Kolb R, Borcherding N, Chatzkel JA, Falzarano SM, et al. Updates on Immunotherapy and Immune Landscape

in Renal Clear Cell Carcinoma. Cancers. 2021; 13: 5856. https://doi.org/10.3390/cancers13225856

[9] Bi K, He MX, Bakouny Z, Kanodia A, Napolitano S, Wu J, et al. Tumor and immune reprogramming during immunotherapy in advanced renal cell carcinoma. Cancer cell. 2021; 39: 649–661. https://doi.org/10.1016/j.ccell.2021.02.015

[10] Makhov P, Joshi S, Ghatalia P, Kutikov A, Uzzo RG, Kolenko VM. Resistance to Systemic Therapies in Clear Cell Renal Cell Carcinoma: Mechanisms and Management Strategies. Molecular Cancer Therapeutics. 2018; 17: 1355–1364. https://doi.org/10.1158/1535-7163.MCT-17-1299

[11] Yang J, Li B, He QY. Significance of prohibitin domain family in tumorigenesis and its implication in cancer diagnosis and treatment. Cell Death & Disease. 2018; 9: 580. https://doi.org/10.1038/s41419-018-0661-3

[12] Artal-Sanz M, Tavernarakis N. Prohibitin and mitochondrial biology. Trends in Endocrinology and Metabolism: TEM. 2009; 20: 394–401. https://doi.org/10.1016/j.tem.2009.04.004

[13] Liu J, Zhang R, Su T, Zhou Q, Gao L, He Z, et al. Targeting PHB1 to inhibit castration-resistant prostate cancer progression in vitro and in vivo. Journal of Experimental & Clinical Cancer Research : CR. 2023; 42: 128. https://doi.org/10.1186/s13046-023-02695-0

[14] Wu TF, Wu H, Wang YW, Chang TY, Chan SH, Lin YP, et al. Prohibitin in the pathogenesis of transitional cell bladder cancer. Anticancer Research. 2007; 27: 895–900.

[15] Jiang L, Dong P, Zhang Z, Li C, Li Y, Liao Y, et al. Akt phosphorylates Prohibitin 1 to mediate its mitochondrial localization and promote proliferation of bladder cancer cells. Cell Death & Disease. 2015; 6: e1660. https://doi.org/10.1038/cddis.2015.40

[16] Guo F, Hiroshima K, Wu D, Satoh M, Abulazi M, Yoshino I, et al. Prohibitin in squamous cell carcinoma of the lung: its expression and possible clinical significance. Human Pathology. 2012; 43: 1282–1288. https://doi.org/10.1016/j.humpath.2011.10.006

[17] Javid H, Hashemy I, Shahidsales S, Mohammadian Roshan N, Kianoosh T, Zahedi Avval F. Tissue Expression of Prohibition-I and It's Relationship With Prognostic Factors in Breast Cancer. Iranian Journal of Pathology. 2018; 13: 237–244.

[18] El-Etreby NM, Ghazy AA, Rashad R. Prohibitin: targeting peptide coupled to ovarian cancer, luteinization and TGF-β pathways. Journal of Ovarian Research. 2017; 10: 28. https://doi.org/10.1186/s13048-017-0325-4

[19] Gregory-Bass RC, Olatinwo M, Xu W, Matthews R, Stiles JK, Thomas K, et al. Prohibitin silencing reverses stabilization of mitochondrial integrity and chemoresistance in ovarian cancer cells by increasing their sensitivity to apoptosis. International Journal of Cancer. 2008; 122: 1923–1930. https://doi.org/10.1002/ijc.23351

[20] Cirilo PDR, de Sousa Andrade LN, Corrêa BRS, Qiao M, Furuya TK, Chammas R, et al. MicroRNA-195 acts as an anti-proliferative miRNA in human melanoma cells by targeting Prohibitin 1. BMC Cancer. 2017; 17: 750. https://doi.org/10.1186/s12885-017-3721-7

[21] Mavila N, Tang Y, Berlind J, Ramani K, Wang J, Mato JM, et al. Prohibitin 1 Acts As a Negative Regulator of Wingless/Integrated-Beta-Catenin Signaling in Murine Liver and Human Liver Cancer Cells. Hepatology Communications. 2018; 2: 1583–1600. https://doi.org/10.1002/hep4.1257

[22] Xu Z, Wu J, Zha X. Up-regulation of prohibitin 1 is involved in the proliferation and migration of liver cancer cells. Science China. Life Sciences. 2011; 54: 121–127. https://doi.org/10.1007/s11427-010-4130-1

[23] Oyang L, Ouyang L, Yang L, Lin J, Xia L, Tan S, et al. LPLUNC1 reduces glycolysis in nasopharyngeal carcinoma cells through the PHB1-p53/c-Myc axis. Cancer Science. 2023; 114: 870–884. https://doi.org/10.1111/cas.15662

[24] Wang H, Zhou Y, Oyang L, Han Y, Xia L, Lin J, et al. LPLUNC1 stabilises PHB1 by counteracting TRIM21-mediated ubiquitination to inhibit NF-κB activity in nasopharyngeal carcinoma. Oncogene. 2019; 38: 5062–5075. https://doi.org/10.1038/s41388-019-0778-6

[25] Liao Q, Guo X, Li X, Xiong W, Li X, Yang J, et al. Prohibitin is an important biomarker for nasopharyngeal carcinoma progression and prognosis. European Journal of Cancer Prevention : the Official Journal of the European Cancer Prevention Organisation (ECP). 2013; 22: 68–76. https://doi.org/10.1097/CEJ.0b013e328354d351

[26] Liu D, Liu Y, Zhu W, Lu Y, Zhu J, Ma X, et al. Helicobacter pylori-induced aberrant demethylation and expression of GNB4 promotes gastric carcinogenesis via the Hippo-YAP1 pathway. BMC Medicine. 2023; 21: 134. https://doi.org/10.1186/s12916-023-02842-6

[27] Jia Y, Liu Y, Zhu J, Liu L, Ma X, Liu D, et al. DEC1 promotes progression of Helicobacter pylori-positive gastric cancer by regulating Akt/NF-κB pathway. Journal of Cellular and Molecular Medicine. 2022; 26: 1943–1954. https://doi.org/10.1111/jcmm.17219

[28] Xing Y, Lin Y, Zhang Y, Hu J, Liu J, Tian Y, et al. Novel cytoplasmic lncRNA IKBKBAS promotes lung adenocarcinoma metastasis by upregulating IKKβ and consequential activation of NF-κB signaling pathway. Cell Death & Disease. 2021; 12: 1004. https://doi.org/10.1038/s41419-021-04304-4

[29] Roe JS, Kim HR, Hwang IY, Cho EJ, Youn HD. von Hippel-Lindau protein promotes Skp2 destabilization on DNA damage. Oncogene. 2011; 30: 3127–3138. https://doi.org/10.1038/onc.2011.40

[30] Chander H, Halpern M, Resnick-Silverman L, Manfredi JJ, Germain D. Skp2B attenuates p53 function by inhibiting prohibitin. EMBO Reports. 2010; 11: 220–225. https://doi.org/10.1038/embor.2010.2

[31] Fusaro G, Dasgupta P, Rastogi S, Joshi B, Chellappan S. Prohibitin induces the transcriptional activity of p53 and is exported from the nucleus upon apoptotic signaling. The Journal of Biological Chemistry. 2003; 278: 47853–47861. https://doi.org/10.1074/jbc.M305171200

[32] McClung JK, Danner DB, Stewart DA, Smith JR, Schneider EL, Lumpkin CK, et al. Isolation of a cDNA that hybrid selects antiproliferative mRNA from rat liver. Biochemical and Biophysical Research Communications. 1989; 164: 1316–1322. https://doi.org/10.1016/0006-291x(89)91813-5

[33] Dart DA, Spencer-Dene B, Gamble SC, Waxman J, Bevan CL. Manipulating prohibitin levels provides evidence for an in vivo role in androgen regulation of prostate tumours. Endocrine-related Cancer. 2009; 16: 1157–1169. https://doi.org/10.1677/ERC-09-0028

[34] van der Mijn JC, Panka DJ, Geissler AK, Verheul HM, Mier JW. Novel drugs that target the metabolic reprogramming in renal cell cancer. Cancer & Metabolism. 2016; 4: 14. https://doi.org/10.1186/s40170-016-0154-8

[35] Hu J, Wang SG, Hou Y, Chen Z, Liu L, Li R, et al. Multi-omic profiling of clear cell renal cell carcinoma identifies metabolic reprogramming associated with disease progression. Nature Genetics. 2024; 56: 442–457. https://doi.org/10.1038/s41588-024-01662-5

[36] Signorile A, Sgaramella G, Bellomo F, De Rasmo D. Prohibitins: A Critical Role in Mitochondrial Functions and Implication in Diseases. Cells. 2019; 8: 71. https://doi.org/10.3390/cells8010071

[37] Ouyang L, Shi Z, Zhao S, Wang FT, Zhou TT, Liu B, et al. Programmed cell death pathways in cancer: a review of apoptosis, autophagy and programmed necrosis. Cell Proliferation. 2012; 45: 487–498. https://doi.org/10.1111/j.1365-2184.2012.00845.

x
[38] Kroeger N, Klatte T, Chamie K, Rao PN, Birkhäuser FD, Sonn GA, et al. Deletions of chromosomes 3p and 14q molecularly subclassify clear cell renal cell carcinoma. Cancer. 2013; 119: 1547–1554. https://doi.org/10.1002/cncr.27947
[39] Gossage L, Eisen T. Alterations in VHL as potential biomarkers in renal-cell carcinoma. Nature Reviews. Clinical Oncology. 2010; 7: 277–288. https://doi.org/10.1038/nrclinonc.2010.42
[40] Li M, Kim WY. Two sides to every story: the HIF-dependent and HIF-independent functions of pVHL. Journal of Cellular and Molecular Medicine. 2011; 15: 187–195. https://doi.org/10.1111/j.1582-4934.2010.01238.x
[41] Fusaro G, Wang S, Chellappan S. Differential regulation of Rb family proteins and prohibitin during camptothecin-induced apoptosis. Oncogene. 2002; 21: 4539–4548. https://doi.org/10.1038/sj.onc.1205551
[42] Wang S, Fusaro G, Padmanabhan J, Chellappan SP. Prohibitin co-localizes with Rb in the nucleus and recruits N-CoR and HDAC1 for transcriptional repression. Oncogene. 2002; 21: 8388–8396. https://doi.org/10.1038/sj.onc.1205944
[43] Wang S, Nath N, Adlam M, Chellappan S. Prohibitin, a potential tumor suppressor, interacts with RB and regulates E2F function. Oncogene. 1999; 18: 3501–3510. https://doi.org/10.1038/sj.onc.1202684
[44] Wang S, Zhang B, Faller DV. Prohibitin requires Brg-1 and Brm for the repression of E2F and cell growth. The EMBO Journal. 2002; 21: 3019–3028. https://doi.org/10.1093/emboj/cdf302
[45] Bacigalupa ZA, Rathmell WK. Beyond glycolysis: Hypoxia signaling as a master regulator of alternative metabolic pathways and the implications in clear cell renal cell carcinoma. Cancer Letters. 2020; 489: 19–28. https://doi.org/10.1016/j.canlet.2020.05.034